
An unstable inner disk in Cyg X-1 ?

Chris DONE and Piotr T. ŻYCKI

*Department of Physics, University of Durham, South Road, Durham
DH1 3LE, England, U.K.*

Abstract

We present the first significant detection of relativistic smearing of the X-ray reflection spectrum from the putative accretion disk in the low/hard state of Cyg X-1. The ionization state, and amount of relativistic smearing are simultaneously constrained by the X-ray spectra, and we conclude that the disk is not strongly ionised, does not generally extend down to the last stable orbit at 3 Schwarzschild radii and covers rather less than half the sky as seen from the X-ray source. These results are consistent with a geometry where the optically thick disk truncates at a few tens of Schwarzschild radii, with the inner region occupied by the X-ray hot, optically thin(ish) plasma. Such a geometry is also inferred from previous studies of the reflected spectrum in Galactic Black Hole transient sources, and from detailed considerations of the overall continuum spectral shape, suggesting that there is some robust instability which disrupts the inner accretion disk in low/hard state Galactic Black Holes.

1. Introduction

Some of the strongest evidence for the existence of black holes has come from recent ASCA (0.6–10 keV) X-ray observations of the shape of the iron $K\alpha$ line in Active Galactic Nuclei (AGN). AGN typically produce copious hard X-ray emission, and the iron line is formed from fluorescence as these X-rays illuminate the infalling material. The combination of Doppler effects from the high orbital velocities and strong gravity close to the black hole gives the line a characteristically skewed, broad profile (Fabian et al., 1989). This has been unambiguously identified in ASCA data from the AGN MCG-6-30-15, where the line width implies that the accretion disk extends down to *at least* $6R_g$ ($R_g = GM/c^2$), the last stable orbit in a Schwarzschild metric (Tanaka et al 1995).

As well as producing the line, some fraction of the illuminating hard X-rays are reflected from the accretion flow, producing a characteristic continuum spectrum. The amplitude of the line and reflected continuum depend on the

amount of material being illuminated by the hard X-rays, its inclination, elemental abundances and ionization state (e.g. Lightman & White 1988; George & Fabian 1991). The amount of reflection and line seen in AGN are consistent with a power law X-ray spectrum illuminating an optically thick, (nearly) neutral disk, which subtends a solid angle of $\sim 2\pi$ (e.g. Pounds et al 1990).

This contrasts with the situation in the Galactic Black Hole Candidates (GBHC). These are also thought to be powered by accretion via a disk onto a black hole, and, in their low/hard state, show spectra which are rather similar to those from AGN. However, the amount of reflection and iron line is much less than would be expected from an accretion disk which subtends a solid angle of 2π (e.g. Gierliński et al 1997), and the detected line is narrow, with no obvious broad component (e.g. Ebisawa et al 1996, hereafter E96). There are (at least) two possible explanations for this: firstly that it is an artifact of a difference in ionization state of the disk between GBHC and AGN, or secondly that there is a real difference in geometry between the supermassive and stellar mass objects.

Ionization differences seems at first sight to be an extremely attractive option. For accretion at the same fraction of Eddington, the disk temperature should scale as $M^{-1/4}$. The GBHC inner disk is then expected to be a factor of ~ 30 hotter than in AGN, and the higher expected ionization state from the thermal ion populations gives a reflected continuum and associated iron line that can be very different to that from a neutral disk (e.g. Ross, Fabian & Brandt 1996). Fits with photo-ionised reflected continua show that the ionization state of the reflector is generally rather low (Done et al 1992; Gierliński et al 1997), arguing against such models. However, relativistic shifts could affect the derived ionization states (e.g. Ross et al., 1996). Here we fit relativistically smeared, ionized models of the reflected continuum to the low/hard state spectra from Cyg X-1 and compare this to data from other GBHC and AGN.

2. Spectral Fitting

We use a reflection model described in detail in Życki et al (1998b), where the iron $K\alpha$ line strength is calculated self consistently with the properties of the reflected continuum, and relativistic effects are then applied to this total reprocessed spectrum. This gives a much more powerful approach than fitting the (relativistically smeared) line and (unsmeared) reflected continuum separately. The free parameters are the solid angle subtended by the reflector to the X-ray source, $\Omega/2\pi$, (an isotropic X-ray source above a flat disk has $\Omega/2\pi = 1$), ionisation state, ξ , and inner radius of the disk R_{in} . We use Morrison & McCammon (1983) abundances, with only iron free to vary from solar $\text{Fe}/\text{H}(= 3.3 \times 10^{-5})$.

2.1. EXOSAT GSPC

The EXOSAT GSPC data from Cyg X-1 give some of the best spectra to date from this object, with the broad 2–20 keV energy range of GINGA data but resolution comparable to that of the ASCA GIS. We use the 5 GSPC spectra of Done et al., (1992). The residuals to a simple power law are shown in Figure 1a, together with the residuals to a simple power law fit to the GINGA-12 AGN spectrum of Pounds et al (1990). Contrary to claims by Ross et al (1996), Cyg X-1 is not dominated by the edge structure, but also shows a strong excess at the iron line energy. *Both* line and edge appear equally diminished in Cyg X-1 compared to AGN.

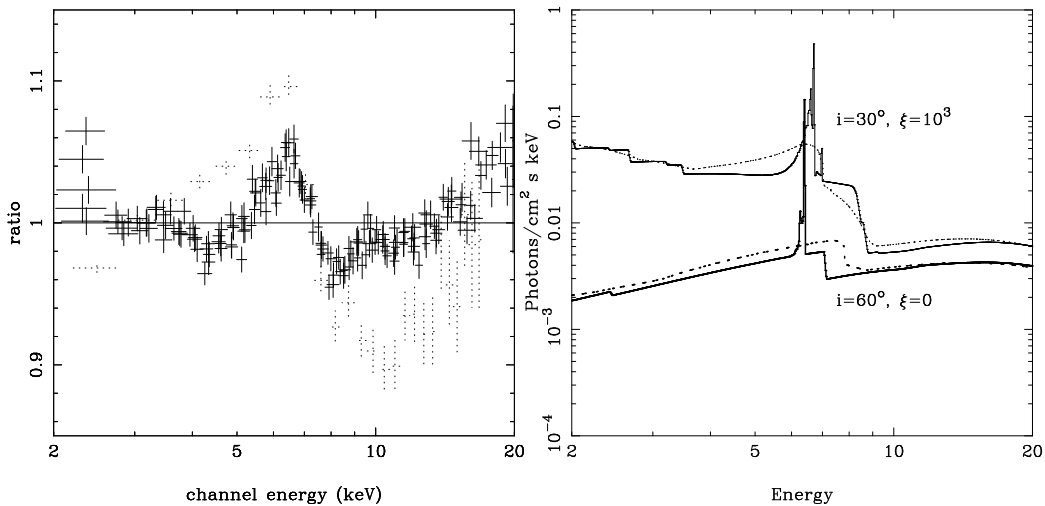


Fig. 1. The left hand panel shows the ratio of the EXOSAT GSPC spectra of Cyg X-1 to a power law model, while the dotted line shows this for the GINGA-12 AGN spectrum (Pounds et al 1990). The right hand panel shows how relativistic smearing and ionization can distort the observed reprocessed spectrum. The thick solid line is the reflected (line and continuum) resulting from power law illumination of a neutral slab inclined at 60° , while the dotted line shows the distortions induced by relativistic effects if the reprocessor is a disk which extends down to the $6R_g$. The thin solid and dotted lines show results for highly ionised ($\xi = 10^3$) material inclined at 30° .

We fit only the data above 4 keV to avoid problems with the soft X-ray excess, and fix the galactic column at $6 \times 10^{21} \text{ cm}^{-2}$. The 5 GSPC spectra are fit simultaneously in XSPEC, although only the reflection parameters of inclination and iron abundance are constrained to be equal across all the datasets. A power law and lightly ionised reprocessed spectrum inclined at 30° gives a good fit

to the data ($\chi^2_\nu = 611/615$), with a derived iron abundance which is close to solar. However, a significantly better fit is obtained if the reprocessed spectrum is relativistically smeared, giving $\chi^2_\nu = 535/604$. The derived inner radius of the disk in each spectrum is generally *inconsistent* with the disk extending down to the last stable orbit, assuming an illumination which is $\propto r^{-3}$, and the derived ionization is rather low with typical values of $\xi \sim 30$, corresponding to FeXII. The iron abundance is now derived to be twice solar, consistent with the abundance of iron inferred for the stellar wind of the companion star from the strong edge feature seen in the absorbed ‘dip’ spectra (Kitamoto et al., 1984). Relativistic smearing allows more iron line to be present, since it is broad rather than narrow, so it is much less observable (see figure 1b). These fits also include an additional (neutral and unsmeared) reprocessed spectrum to allow for a contribution from the companion star and/or outer disk (Basko 1978); such narrow features are detected in high resolution data (e.g. E96) although they are not significant in the EXOSAT data.

2.2. ASCA GIS and SIS

This model (power law, relativistically smeared reprocessed spectrum, and unsmeared reprocessed spectrum) was also fit to the 4–10 keV ASCA GIS and SIS datasets of E96. The 8 ASCA GIS spectra can again be fit simultaneously, with only the reflected parameters of abundance and inclination tied across the datasets. A power law and an unsmeared reflected spectrum inclined at 30° give $\chi^2_\nu = 951.9/647$. The derived reflected spectra are all lightly ionised, again with typical $\xi \sim 30$. The situation changes dramatically when relativistic smearing is included, along with an unsmeared, unionised reflected component from the companion star. The fit is clearly statistically significantly better – χ^2_ν drops to 753/632. However, the derived ionisation state of the relativistic reflector is very high, typically with $\xi \sim 10^{3-4}$. Figure 2a shows the best fit to one of the ASCA GIS spectra (3). The ionisation is so extreme that the ‘edge’ feature seen in the data is actually modelled by the end of the relativistically smeared ionised line, and the real edge is shifted out of the observed energy range. Similar results are seen for most of the ASCA GIS and SIS spectra.

2.3. Inclination

This general mismatch between the ionization of the reprocessor derived from ASCA and EXOSAT data is suggestive of a systematic problem in the spectral model fitting, most likely due to the difference in bandpass. In EXOSAT the high energy continuum shape of the reprocessed spectrum helps constrain its ionization, whereas in ASCA only the iron features can be used. The detailed

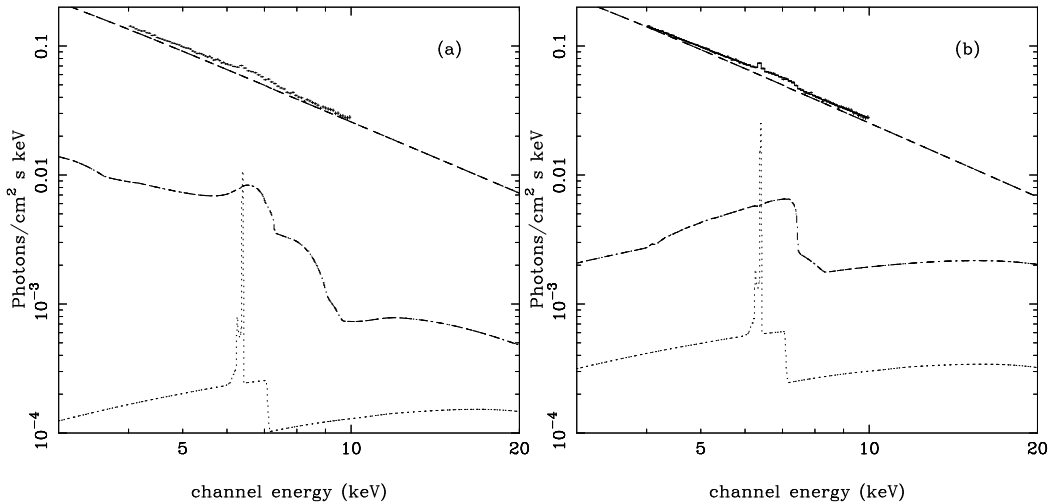


Fig. 2. Panel (a) shows the best fit to the ASCA GIS 3 spectrum with a relativistic disk inclined at 30° . The derived ionisation state of the reflector is extreme with $\xi = 3.0 \pm 2.4 \times 10^4$, for solid angle $\Omega/2\pi = 0.06_{-0.02}^{+0.03}$ and inner disk radius of $58_{-31}^{+110} R_g$ ($\chi_\nu^2 = 92/79$). The right hand panel shows the significantly better ($\chi_\nu^2 = 69.8/79$) higher inclination 53° solution for the GIS 3 data, which has $\Omega/2\pi = 0.53_{-0.17}^{+0.09}$, an inner radius of $9.9_{-1.9}^{+6} R_g$ and $\xi = 0^{+17}$. This corresponds much better to the EXOSAT solutions, which always pick a low ionisation reflector, irrespective of inclination.

shape of the line and edge is a strong function of inclination as well as of ionization. At high inclinations Doppler shifts prevail over gravitational and transverse redshift, shifting the line and edge to higher energies as well as giving substantial broadening. This is to zeroth order the same effect as ionisation. However, the detailed shape of a low inclination, ionised reflection spectrum is rather different to a less ionised reflection spectrum at higher inclination, so these two parameters can be disentangled given good enough data.

Figure 3a shows how χ^2 varies as the inner disk inclination changes from $30 - 66^\circ$ for the GSPC data, while Figure 3b shows this for the ASCA GIS 3 spectrum data. Clearly there is a significant preference in the data for an inclination higher than 30° (cosine smaller than 0.86), with a best fit at $\sim 53^\circ$. This is rather higher than the inclination of $28 - 38^\circ$ inferred from optical studies, although within their firm upper limit of 55° (Sowers et al 1998). We fit all the EXOSAT and ASCA spectra with a relativistic reprocessor inclined at $\sim 53^\circ$. This gives similar derived ionization for both sets of data, with typical values of $\xi \leq 20$, corresponding to \leq FeX. Figure 2b shows this high inclination fit to the

GIS 3 spectrum. This is a substantially better description ($\Delta\chi^2 \sim 20$) of the data than the fit assuming a disk inclined at 30° .

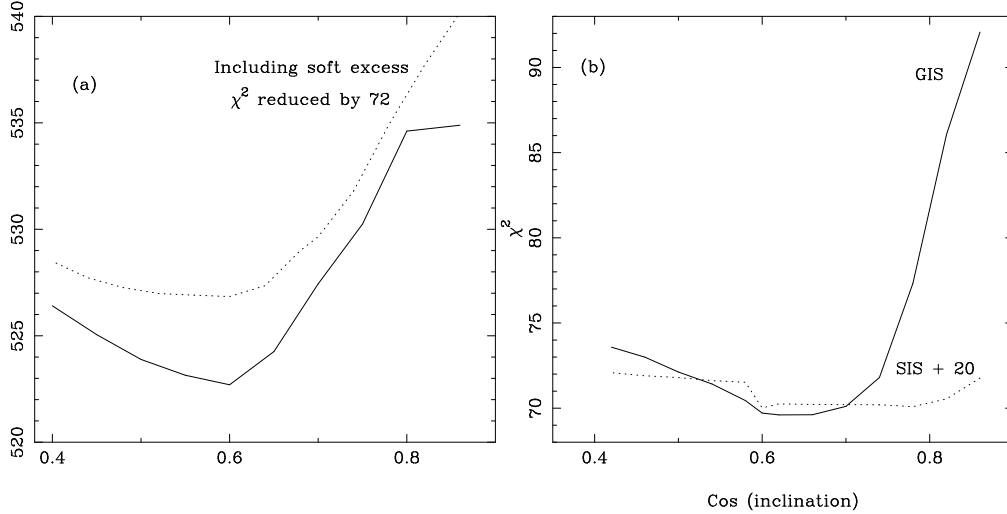


Fig. 3. The change in χ^2 (goodness of fit parameter) as a function of inclination of the reflecting material. Panel (a) shows results from a simultaneous fit of all the EXOSAT GSPC spectra, with the solid line showing fits to the data from 4–20 keV while the dotted line uses the full 2–20 keV bandpass including a (diskblackbody) model for the soft excess. Panel (b) shows the ASCA GIS 3 (solid line) and ASCA SIS 5 (dotted line) 4–10 keV spectral results.

For both the EXOSAT and ASCA data, the high inclination fits have a derived inner disk radius of $10 - 20R_g$, generally *inconsistent* with the optically thick material extending down to the innermost stable orbit at $6R_g$ (Done & Życki 1998). A similar 'hole' in the inner disk is also seen from the detailed reflected spectral shape of low/hard spectra from other GBHC (Życki et al., 1997; 1998ab), implying that there is some robust physical mechanism which disrupts the flow.

3. AGN: MCG–6–30–15

We use our model to fit the seminal ASCA data from the AGN MCG–6–30–15, in order to compare with our results from Cyg X–1 and the other GBHC. Published data usually concentrate on the ASCA SIS spectrum since this has the highest spectral resolution. However, the time dependent corrections to the gain of the SIS detectors due to radiation damage are not well understood and these problems have been exacerbated by software errors (<http://heasarc.gsfc.nasa.gov/docs/asca/rddrecipe.html>). Hence we fit the two GIS spectra from MCG–6–30–15. We use

a spectral model with a power law continuum and its relativistic reflection, together with two ionised absorbers in the line of sight (see e.g. Otani et al 1997). Figure 4a shows the resulting fit which has a rather steep intrinsic power law, with $\Gamma = 2.11_{-0.05}^{+0.14}$, an inner disk radius of $R_{\text{in}} = 6^{+1}R_{\text{g}}$, and $\Omega/2\pi_{\text{rel}} = 0.9_{-0.3}^{+0.4}$, with derived iron abundance of $3.7_{-2.3}^{+6.3}$ ($\chi^2_{\nu} = 1343/1308$). Plainly our code is capable of seeing a highly relativistic disk, so the absence of the extreme relativistic components in Cyg X-1 and the other GBHC is not due to our model assumptions. As a cautionary note, we also include the SIS 0 spectrum of MCG-6-30-15 compared to the best fit GIS model (Figure 4b): the discrepancies are obvious.

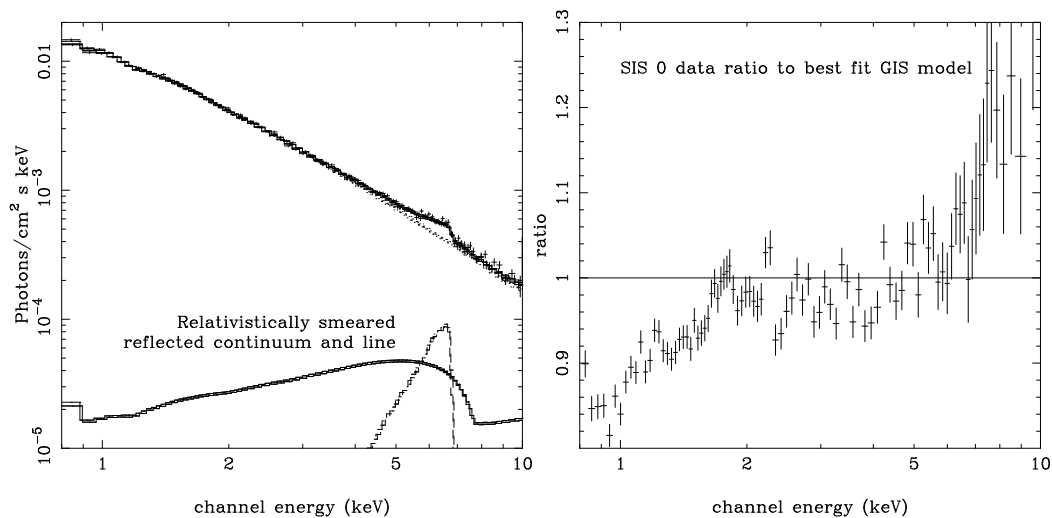


Fig. 4. The left hand panel shows the best fit 30° inclination relativistic disk model for the GIS data from the AGN MCG-6-30-15. The right hand panel shows the ratio of this fit with the SIS 0 data.

4. Conclusions

We significantly detect relativistic smearing of the reprocessed features in Cyg X-1, and find that the disk is not highly ionised. The line is not suppressed relative to the reflected continuum, it is merely broadened by the relativistic effects which made it difficult to detect in ASCA data (E96), where the observed weak and narrow line emission probably comes from the companion star. The derived covering fraction of the relativistic reflector is substantially less than expected from a flat disk. The most plausible explanation for these observations is that the optically thin(ish) X-ray corona fills a central ‘hole’, so that less than half of the X-ray flux intercepts the disk. Similar geometries are derived from energetic arguments about the continuum shape (see e.g. Poutanen 1998).

But what causes such a 'hole' in the inner disk ? The geometry is qualitatively (but not quantitatively) consistent with the advective flow models proposed by Esin et al., (1997; 1998). But is it really an advective flow ? The Esin et al (1997) models identify the soft-hard state transition with the critical accretion rate at which the advective flows can exist. The disk then has a constant efficiency at converting mass to radiation in the soft state ($L \propto \dot{M}$), which then changes to $L \propto \dot{M}^2$ for the advective flow (as these have a lower radiative efficiency at lower density). The *constant decay timescale* of the FRED soft X-ray transients seems then to strongly argue against such models. And what happens to the inner disk in the AGN ? Does it always extend down to $6R_g$, as in MCG-6-30-15 i.e. is the inner disk instability suppressed in AGN ? Or is MCG-6-30-15 an extremum in the distribution of inner disk radii, as suggested by Zdziarski et al (1998). What is the nature of the accretion flow onto a black hole ?

5. References

- Basko M.M., 1978, ApJ., 223, 268
 Done C., Mulchaey J.S., Mushotzky R.F., Arnaud K.A., 1992, ApJ., 395, 275
 Done C., Życki P. T. 1998, MNRAS, submitted
 Ebisawa K., Ueda Y., Inoue H., Tanaka Y., White, N.E. 1996, ApJ., 467, 419
 Esin A. A., McClintock J. E., Narayan R. 1997, ApJ 489, 865
 Esin A. A., Narayan R., Cui W., Grove J. E., Zhang S.-N. 1998, ApJ 505, 854
 Fabian A.C., Rees M.J., Stella L., White, N.E. 1989, MNRAS, 238, 729
 George I.M., Fabian A.C., 1991, MNRAS, 249, 352
 Gierliński M. et al. 1997, MNRAS 288, 958
 Kitamoto S., et al., 1984, PASJ, 36, 799
 Lightman A.P., White T.R., 1988, ApJ, 335, 57
 Morrison R., McCammon D., ApJ., 270, 119
 Otani C., et al., 1997, PASJ, 48, 211
 Pounds K.A., et al., 1990, Nature, 344, 132
 Poutanen J. 1998, in Theory of Black Hole Accretion Discs, eds. M. A. Abramowicz, G. Björnsson, J. E. Pringle (CUP, Cambridge) (astro-ph/9805025)
 Ross R.R., Fabian A.C., Brandt W.N., 1996, MNRAS, 278, 1082
 Sowers J.W., et al., 1998, ApJ., 505, 424
 Tanaka Y. et al. 1995, Nature, 375, 659
 Zdziarski A.A., Lubiński P., Smith D.A., 1998, MNRAS, submitted
 Życki P. T., Done C., Smith D. A. 1997, ApJ 488, L113
 Życki P. T., Done C., Smith D. A. 1998a, ApJ 496, L25
 Życki P. T., Done C., Smith D. A. 1998b, MNRAS, submitted (astro-ph/9811106)